INDONESIAN JOURNAL OF INNOVATION AND APPLIED SCIENCES (IJIAS)
Journal Homepage: https://ojs.literacyinstitute.org/index.php/ijias
E-ISSN: 2775-4162

Volume 6	Issue 1	February (2026)	DOI: 10.47540/ijias.v6i1.2649	Page: 103 – 116

Deflection behavior and fixity point location of piles in soft soil in Banjarmasin due to lateral force

Ainul Mardiyah[1], Rustam Effendi[1]
[1]Civil Engineering Department, University of Lambung Mangkurat, Indonesia
Corresponding Author: Ainul Mardiyah; Email: 2220828320066@mhs.ulm.ac.id

ARTICLE INFO

Keywords: Deflection, Eccentricity, Fixity Point, Lateral Force.

Received : 14 January 2026
Revised : 11 February 2026
Accepted : 24 February 2026

ABSTRACT

Piles sometimes have to bear lateral loads that can generate lateral forces. These lateral forces cause deflections that can affect the position of the fixity point. Therefore, in this study, a modeling test was conducted to analyze the effect of pile stiffness (EI) variations on deflection values and fixity point locations. The research method involved creating a small-scale pile model with varying dimensions and specific loads. A test specimen in the form of a pile was subjected to lateral loads, and the deflection was then measured. The test results were further analyzed using MATLAB software to carefully analyze the pile deflection points and read the position of the fixity point. After conducting the research, it was concluded that the effect of pile stiffness (EI) variation on the deflection value for EI1 = 0.00012 kNm^2 ranges from 0.19D to 0.86D; EI2 = 0.0003 kNm^2 ranges from 0.16D to 0.66D, and EI3 = 0.00062 kNm^2 ranges from 0.09D to 0.44D. The fixity point values range from EI1 = 0.00012 kNm^2 ranging from 12.5D – 17.3D; EI2 = 0.0003 kNm^2 ranging from 12D to 14D and EI3 = 0.00062 kNm^2 ranging from 10.5D to 12D. Also, the eccentricity distance to the fixity point location value ranges from 3e to 3.6e, and the deflection value ranges from 0.1e to 0.17e.

INTRODUCTION

Banjarmasin is the capital and largest city in South Kalimantan Province. The development of infrastructure in Banjarmasin includes high-rise buildings, bridges, port facilities, and other civil engineering structures. Where high resistance against lateral loads are required (Jeong, 2020). The soil profile and depth of each layer of soil is not the same for every place (Moayedi, 2018). Most of these structures are supported by pile foundations due to the soft soil conditions. Pile foundations are commonly designed to resist not only vertical loads but also lateral loads. Lateral loads may be caused by wave action, river currents, wind forces, and earthquake effects. More powerful lateral loads occur as a result of unpredictable events such as heavy wind, earthquakes, slope failure, and lateral spread induced by liquefaction (Jegatheeswaran, 2016).

These lateral forces can induce horizontal deflection of piles and influence the depth of the fixity point. Therefore, the analysis of laterally loaded piles is essential in foundation design because lateral loads significantly affect pile behavior and structural stability. When designing pile foundations under lateral loading, the interaction of the piles with the surrounding soils is crucial (Nimityongskul, 2018). Depending on the pile's position within the group and its lateral deflection, the main elements influencing the change in the lateral resistance of piles are the increase and decrease in lateral stress in clayey soils, respectively (Hazzar, 2017).

The point-of-fixity method is widely used as a common design practice where the complex interaction between soil and deep foundation under lateral load is sought to be replaced by an equivalent, fixed-based cantilever model. Recent studies attempted to propose more robust procedures to calculate depth-to-fixity, depending on various factors affecting the nonlinear lateral response of the soil-foundation system, as opposed

to using empirical equations from design codes. This study proposes a simple method to determine depth-to-fixity, based on an analytical solution to the equivalent cantilever model (Bhuiyan, 2024).

Pile failure under lateral loading may occur due to the failure of either the soil or the pile. The failure mechanism is known as rigid-pile (or short pile) failure if it results from the soil surrounding the embedded pile length yielding. However, the failure mechanism is flexible pile (also known as extended pile failure) if the failure results from the pile section itself yielding at the location of the highest moment (Abdelaziz, 2021). Specifically, the complicated soil-structure interaction issue is the problem of laterally loaded piles. Building frames are supported by raft or mat foundations, pile foundations, isolated footings, or combination footings. When lateral loads from a foundation system are taken into consideration, the analysis gets more complex (Jagtap, 2017). Long piles have very high passive resistance and are unable to tilt or rotate. The upper component deflects in flexure, whereas the lower part stays almost vertical because of fixity. When a plastic hinge forms at the maximum bending moment, the pile collapses. When the long pile's capacity is exceeded, structural failure occurs (Rad, 2017).

Lateral forces may arise from several sources, including soil pressure acting on retaining structures, wind loads, seismic loads, and eccentric loading on columns (Aulia, 2019). When lateral loads act on a structure supported by pile foundations, they can induce horizontal displacement and cause stress redistribution in the surrounding soil. If the applied lateral load exceeds the allowable soil resistance, soil yielding may occur around the pile, leading to excessive lateral deflection beyond the permissible limit. This condition indicates that the load has surpassed the soil bearing capacity and may result in foundation instability (Rawung, 2020).

The geological conditions in Banjarmasin are generally dominated by soft soil deposits that are widely distributed across the area. Soft soils, particularly clay and peat, present significant challenges for construction due to their unfavorable engineering characteristics. These soil types are not ideal for supporting structural loads and frequently lead to geotechnical problems such as excessive settlement and low bearing capacity. The engineering properties of soft soils typically include low shear strength, high compressibility, low bearing capacity, and low California Bearing Ratio (CBR) values. Such characteristics make soft soils unsuitable for shallow foundation systems and often require special ground improvement or deep foundation solutions (Darmawandi, 2020).

It is well known that for a laterally loaded slender pile in clay, two soil failure mechanisms may exist. In the upper part, soil fails in a conical wedge that extends to the soil surface. A gap may also form along the interface between the pile and the soil on the active side if the suction between the pile and the soil is lost. At a certain depth, however, the soil failure mechanism transits into a localized plane flow-around mechanism, as the soil resistance encountered in this mechanism becomes less than failure in a conical wedge (Zhang, 2017).

To simulate actual field conditions, this study was conducted using a small-scale physical model to represent the behavior of pile foundations subjected to lateral loading. The model was designed to provide a general understanding of pile response under horizontal forces. Through this experimental approach, it becomes possible to estimate the magnitude of lateral deflection and to determine the location of the fixity point along the pile shaft. The results are expected to contribute to predicting pile performance in soft soil conditions, particularly for structures constructed in Banjarmasin.

METHODS

The study commenced with the design and fabrication of a physical model in the laboratory to simulate pile behavior under controlled conditions. The experimental program was carried out in several sequential stages, starting from material preparation and model assembly to the application of lateral loading and measurement of pile response. The stages of model development and laboratory testing are presented as follows.

Model creation

After determining the modeling design, the next step is to create the modeling tools, as follows:

1. Fabricate a rectangular acrylic container with dimensions of 13 cm × 12 cm × 30 cm using 5 mm thick acrylic sheets.
2. b. Install a wooden base beneath the acrylic container and secure it firmly using bolts to

ensure structural stability.

3. Attach wooden reinforcement frames along each side of the acrylic walls to enhance the rigidity and overall strength of the container.
4. Mount a wooden block at the upper left side of the container. Subsequently, drill aligned holes on both sides of the block to accommodate the insertion of iron rods used in the loading mechanism.
5. These rods are used to hang the weights.
6. The weights used are 50 g, 100 g, 150 g, and 200 g.
7. Install a dial on the upper right side of the box to read the deflection value.
8. Provide a reference point on the front of the acrylic to measure the deflection at each depth y.
9. Make pile models with sizes of 4 mm, 5 mm, and 6 mm with lengths of 20 cm, 25 cm, and 30 cm, respectively.

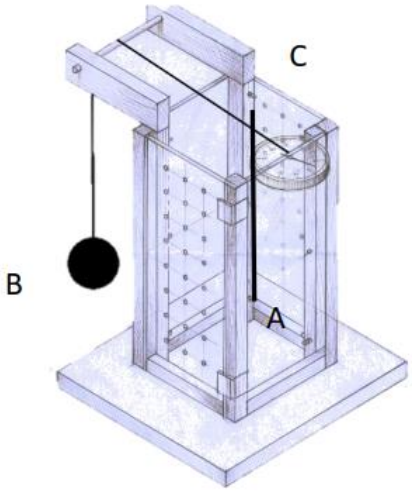

Figure 1. Model Sketch

Description:
A: Pile
B: Load
C: Dial

Figure 2. Test Box

Model testing

1. Weigh 5 kg of soil according to the weight-volume equation.
2. Then saturate the soil by adding water and soaking it for
3. 24 hours.
4. Then put the soil into an acrylic box and compact it.
5. Put the soil into the box gradually (in 10 cm layers) to facilitate even distribution. Each layer is slowly leveled so that there are no air pockets between the soil layers.
6. Each layer of soil is compacted manually using a small tamper or other tools until the surface appears dense and stable. The goal is to ensure that the density of all soil layers is uniform and in accordance with field conditions.
7. After the soil is compacted, conduct a soil density test using a vane shear test device 3 times to determine the su value that is close to the Su value in the field.
8. Install the test pile according to the research variation, then set the dial to zero and place the load on the pile.
9. Take a photo of the pile model before testing.
10. Read the deflection on the dial on the pile.
11. The deflection reading is the final reading until there is no further movement.
12. Take a photo of the pile model after testing.
13. Compact the soil again, then continue with the next load.

RESULTS AND DISCUSSION

The results of the soil's mechanical and physical testing indicate that the values are within the range of soft soil. Table 1 presents the results of physical and mechanical tests.

Table 1. Physical and Mechanical Properties of Soft Soil in Banjarmasin

Parameter		Units	Value
Soil Properties	Soil Unit Weight	gr/cm^3	1,5
	Specific Gravity (Gs)		2,742
	Water Content	%	98,63
Atterberg Limits	Liquid Limit (LL)	%	68,21
	Plastic Limit (PL)	%	31,11
	Plasticity Index (PI)	%	37,10
	Soil Classification		CH
Grain Size Distribution	Gravel (>2 mm)	%	0,57
	Coarse Sand (0.6-2.00mm)	%	0,5
	Medium Sand (0.2-0.6mm	%	0,57
	Fine Sand (0.05-0.2mm)	%	7,21
	Silt and Clay (0.002-0.05)	%	72,23
	Clay (<0.002mm)	%	18,92
	Percent Passing		
	No.10 (2.00mm)	%	99,43
	No.40 (0.425mm)		98,73
	No.200 (0.0075mm)		98,03
Direct Shear Test	Cohesion *c*	Kg/cm^2	0,0959
	Friction Angle ø	^{o}	5,48
Vane Shear Test	Undrained Shear Strength (Su)	kPa	10
Unconfined Compression Test	Unconfined Compressive Strength (qu)	Kg/cm^2	0,1786
	Strain (ε)	%	9,625
	Sensitivity (St)		1,2386
	Cohesion (c)	Kg/cm^2	0,0893

According to Table 1, the soft soil in Banjarmasin has physical and mechanical characteristics dominated by fine-grained fractions. The soil employed in this test is categorized as soft soil with a preponderance of fine grains based on the findings of laboratory analysis. According to the findings of the particle distribution, the silt and clay fractions make up 91.15%, with 72.23% silt and 18.92% clay, respectively. This soil is nearly exclusively composed of small particles, as evidenced by the fact that the total sand content is only 8.28% and the gravel concentration is 0.57%. The soil has highly fine-grained properties, as evidenced by the fact that 98.03% of the soil particles went through a No. 200 sieve (0.0075 mm). This type of soil typically has strong plasticity, low permeability, compressible qualities, and is readily consolidated under load.

The soil's physical state also reveals a very high water content of 98.63%, suggesting that it is nearly saturated. Furthermore, the comparatively low bulk density of the soil, 1.5 g/cm³ (15 kN/m³), supports the idea that the soil is soft and has wide, water-filled pores. A comparatively low density that is compatible with soft soil is shown by the soil's specific gravity of 2.742 and bulk density of 1.5 g/cm³ (Bowles, 1997). According to mechanical metrics, the soil has a limited lateral bearing capacity and is prone to deformation, as evidenced by its undrained shear strength (Su) of 10 kPa and soil elasticity modulus of 128 kPa.

The results of the modeling tests in the Laboratory are shown in Figures 3 and 4. These figures illustrate the deflection and fixity point results according to variations in the length and diameter of the pile.

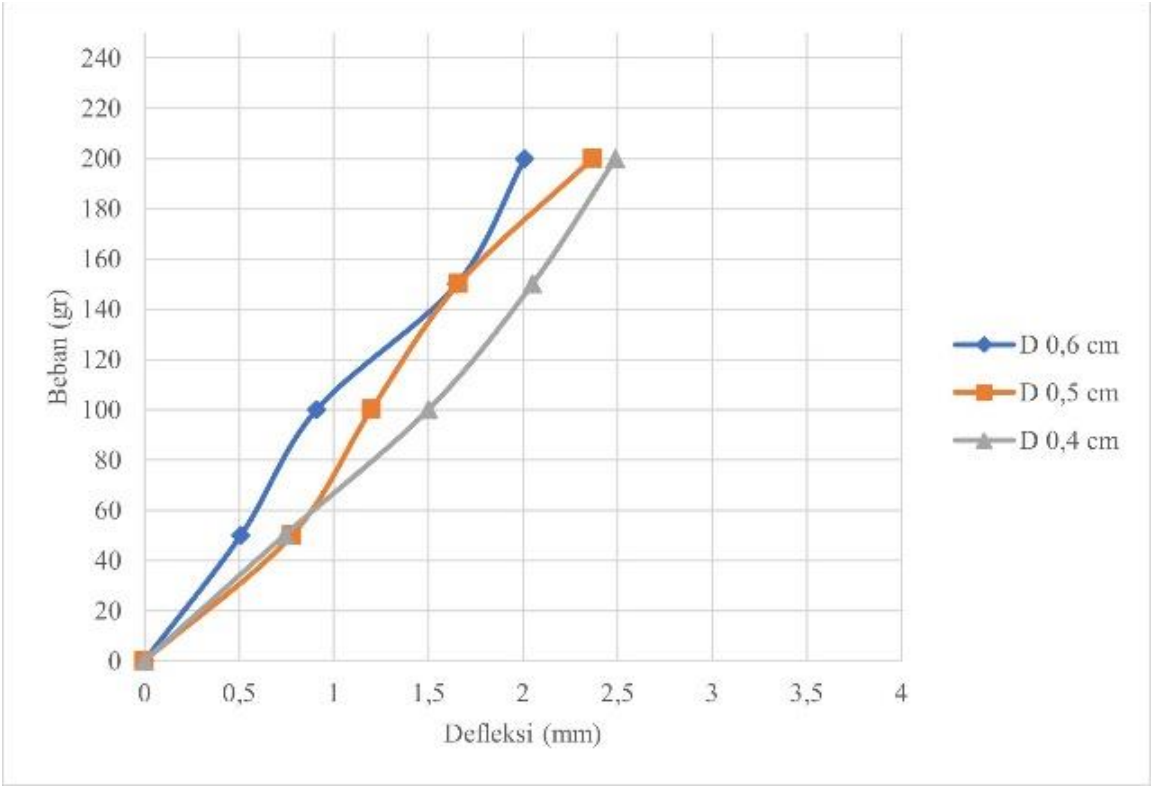

Figure 3. Correlation between load (gr) and deflection (mm) at the dial tip on the pile (P = 30 cm)

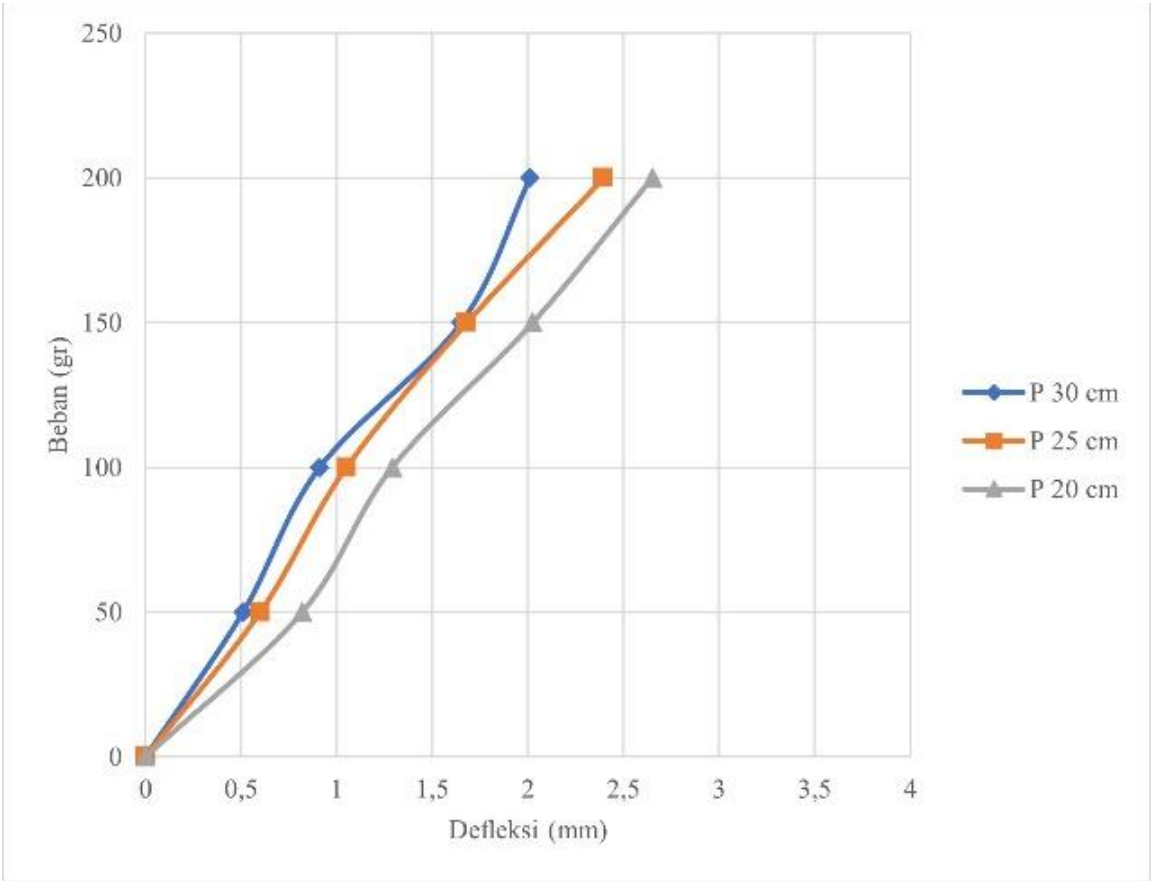

Figure 4. Correlation between Load (gr) and Deflection (mm) at the dial tip on the pile (D = 0,4 cm)

Figures 3 and 4 demonstrate that a pile's length increases with its diameter, and that the deflection value generated increases with the load. The graph line, which rises linearly, illustrates this. This is consistent with the study's findings that, when supported by soft soil, longer, thinner rods are more prone to bending deformation because to their lower EI stiffness. (Kavitha, 2016; Boudaa, 2019). The deflection rises as the beam's length increases and falls as its diameter increases. It is observed that the horizontal displacement increases along with the increasing horizontal load (Lu, 2017).

To locate the fixity point on the picture of the pile model test in the lab, image reading is done. The outcomes of laboratory tests using a pile length of 30 cm and a diameter of 4 mm under a load of 200 gr are displayed in Figure 5. The corresponding program is compiled through MATLAB software (Zhang, 2021). MATLAB software will read the image from the photo. It is evident from the image that the pile changes after loading when tested for a pile length of 30 cm with a diameter variation of 4 mm. This indicates that the pile is displaced or deflected by a distance of x from the beginning point.

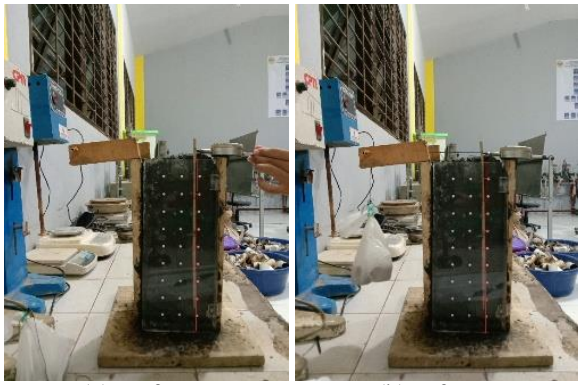

(a) Before (b) After

Figure 5. The length of the pile is 30 cm and the diameter is 0.4 mm at a load of 200 gr.

Table 2 shows the results of pixel measurements on the image (photo) in Figure 5, which then illustrates the deformation of the pile in Figure 6. The pixel values are converted to units of length in millimeters. The following are the details of the test results on the model pile with a length of 30 cm and a diameter of 4 mm.

Table 2. Pile displacement data

No.	First (pixel)		Final (pixel)	
	x	y	X	Y
1	2090.9	1523.2	2075.4	1523.2
2	2090.9	1749.3	2088.2	1759.3
3	2090.9	1939.1	2090.5	1947
4	2090.9	2126	2090.8	2131.7
5	2090.9	2321.4	2090.6	2325.1
6	2090.9	2513.9	2090.8	2515.6
7	2090.9	2706.5	2090.8	2709
8	2090.9	2882.3	2090.8	2896.6
9	2090.9	3083.2	2090.8	3078.5
10	2090.9	3270.2	2090.8	3269
11	2090.9	3405.8	2090.8	3403.8

Based on the data in Table 2, which is then scaled from pixels to millimeters. The data in Table 3 represents the displacement values that have been scaled to millimeters.

Table 3. Coordinate Point

No.	First (mm)		Final (mm)	
	x1	y1	x2	y2
1	0.00	0.00	-2.47	0.00
2	0.00	36.02	-0.43	36.02
3	0.00	66.26	-0.06	66.26
4	0.00	96.03	-0.02	96.03
5	0.00	127.16	-0.05	127.16
6	0.00	157.83	-0.02	157.83
7	0.00	188.51	-0.02	188.51
8	0.00	216.52	-0.02	216.52
9	0.00	248.53	-0.02	248.53
10	0.00	278.32	-0.02	278.32
11	0.00	299.92	-0.02	299.92

The data in Table 3 were then plotted on a graph showing the pile deflection profile, as shown in Figure 6. The graph illustrates the pile deflection before loading (initial) and after loading (final).

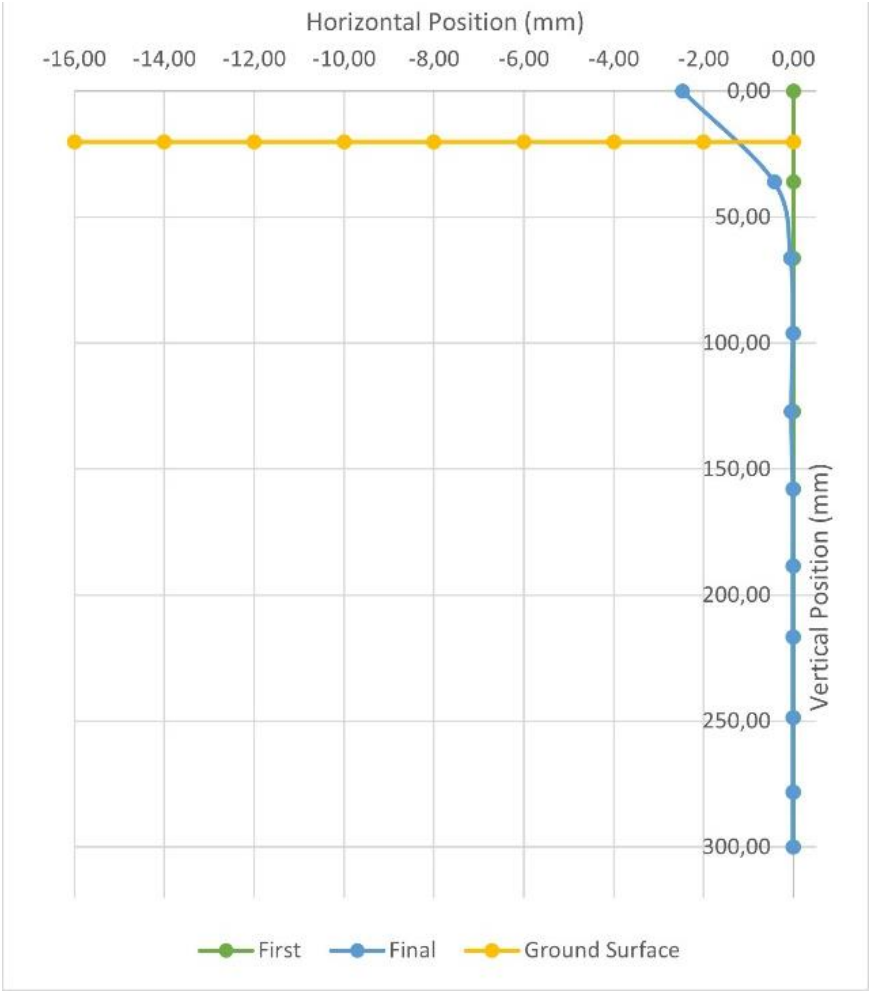

Figure 6. Pile deformation profile

In the pile deformation profile image in the Figure 6, the deflection of the test pile is seen to curve at the top to a depth of 50 mm from the ground surface and then straighten thereafter. The point of change from curved to straight is taken as the fixity point. A deflection value of 2.47 mm was obtained with a pile stiffness (EI) = 0.00012 kNm^2 and soil modulus (E) = 3000 kPa. With a pile diameter of 4 mm and a pile length of 30 cm, the pile experienced a decrease in deflection value and an increase in the distance of the fixity point. This is because the increased dimensions of the column significantly affect the deflection value and the point of deflection. The smaller the stiffness, the smaller the deflection value and the point of deflection. The negative values on the graph indicate that the column deflects to the left.

Table 4 contains the results of Broms' theoretical fixity point calculations compared with the fixity point results from the MATLAB readings.

Table 4. Calculation results of the fixity point

No.	P (cm)	D (mm)	EI (kNm^2)	Zf (mm)
1	20	4	0.00012	64,65
2	20	5	0.0003	94,09
3	20	6	0.00062	115,08
4	25	4	0.00012	65,07
5	25	5	0.0003	91,74
6	25	6	0.00062	110,50
7	30	4	0.00012	56,53
8	30	5	0.0003	82,17
9	30	6	0.00062	103,19

The data in Table 4 were then plotted on a graph showing the deflection profile of the pile, as shown in Figure 7, to compare the positions of the fixing points before loading (initial) and after loading (final)—which are the laboratory results—with the theoretical calculations.

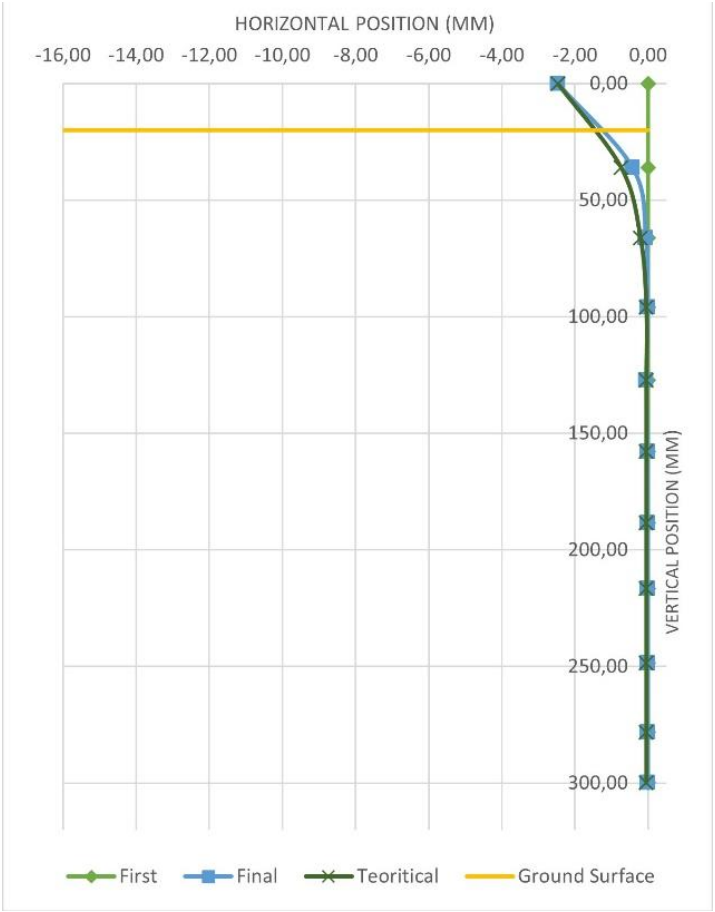

Figure 7. Pile Deformation Profile for Lateral Load = 200 g at length variation = 30 cm diameter = 4 mm

In the pile deformation profile image in Figure 7, the deflection of the test pile is seen to curve at the top to a depth of 50 mm for the laboratory test and 56,53 mm for teoretical calculation from the ground surface and then straighten thereafter. The point of change from curved to straight is taken as the fixity point.

To facilitate practical implementation, the deflection values and fixity point locations were expressed in normalized form, either without dimensional units or in terms of constant coefficients as stated in Table 5 and Table 6. This approach allows the results to be applied more generally to various pile dimensions. The application procedure is carried out by establishing a relationship between the pile diameter and specific parameters, such as the diameter multiplication factor, which can be used as a reference to determine the corresponding fixity point and lateral deflection values.

Table 5. Comparison of deflection values at a load of 200 grams

No.	Dimension		EI	Deflection (mm)			δ/D		
	P (cm)	D (mm)	(kNm^2)	Lab	MATLAB	Theoritical	Lab	MATLAB	Theoritical
1	20	4	0.00012	3.37	3.36	1,50	0.84	0.84	0.38
2	20	5	0.0003	3.30	3.25	1,88	0.66	0.65	0.38
3	20	6	0.00062	2.65	2.64	2,25	0.44	0.44	0.38
4	25	4	0.00012	3.42	3.35	1,50	0.86	0.84	0.38
5	25	5	0.0003	3.10	3.00	1,88	0.62	0.60	0.38
6	25	6	0.00062	2.39	2.33	2,25	0.40	0.39	0.38
7	30	4	0.00012	2.49	2.47	1,50	0.62	0.62	0.38
8	30	5	0.0003	2.37	2.34	1,88	0.47	0.47	0.38
9	30	6	0.00062	2.01	1.99	2,25	0.34	0.33	0.38

Table 6. Comparison of deflection values at a load of 200 grams

No.	Dimensi		EI	Fixity Point (mm)		z/D		zf/e (e = 20 mm)	δ/e (e = 20 mm)
	P (cm)	D (mm)	(kNm^2)	Lab	Theoritical	Lab	Theoritical		
1	20	4	0.00012	69	64,65	17,3	16,2	3,5	0.17
2	20	5	0.0003	60	94,09	12,0	18,8	3,0	0.17
3	20	6	0.00062	63	115,08	10,5	19,2	3,2	0.13
4	25	4	0.00012	60	65,07	15,0	16,3	3,0	0.17
5	25	5	0.0003	63	91,74	12,6	18,3	3,2	0.16
6	25	6	0.00062	66	110,50	11,0	18,4	3,3	0.12
7	30	4	0.00012	50	56,53	12,5	14,1	2,5	0.12
8	30	5	0.0003	70	82,17	14,0	16,4	3,5	0.12
9	30	6	0.00062	72	103,19	12,0	17,2	3,6	0.10

Tables 5 and 6 contain the deflection and fixity point values of the piles, which have been converted into dimensionless constants to facilitate the description of these values. These values were then plotted on graphs showing the relationship between the EI stiffness and the deflection and fixity point constants as a function of the pile diameter. These graphs can be seen in Figures 8 and 9.

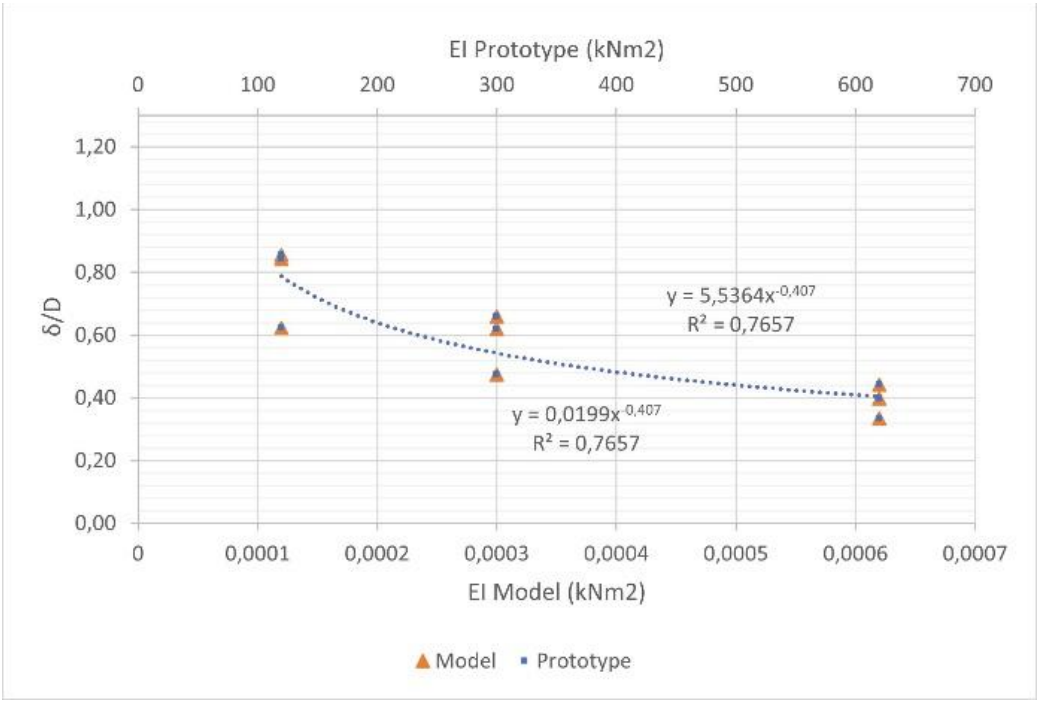

Figure 8. Application of Stiffness Values to Deflection

Figure 8 shows the relationship between the flexural stiffness value (EI Model) and the relative deflection ratio (δ/D) for the Model and Prototype conditions. The graph indicates that an increase in the EI value results in a decrease in the relative deflection ratio, suggesting that as structural stiffness increases, the resulting deflections decrease.

The deflection values for laboratory results, MATLAB, and theoretical values are quite close. The laboratory deflection values range from 0.09D to 0.86D, the MATLAB deflection values range from 0.09D to 0.84D, and the theoretical value is 0.38D. This is in line with research (Yin, 2018) that parametric studies were performed, and it shows that horizontal displacement, rotation, bending moment, and shear force increase along with increasing slope angles; the depth of maximum moment is locates at about 1.6D belowground surface for horizontal ground. Furthermore, Li (2020) states that for the same combination of vertical and lateral stresses, the head displacement of the pile with fixed head and free base conditions

is significantly less than that with free head and free base.

The cohesive surface layer was where most of the lateral displacement that was seen took place. Additionally, it is noted that for front rows, the minimum deflection in each pile is between 4 and 5 m (13–16D) below the ground surface, whereas for middle and back rows, the minimum deflection is between 2 and 3 m (6.5–9.8D) below the soil surface (Deendayal, 2018). Another source of resistance is the lateral friction force on the monopile tip, which can reach a peak value of up to 20% of the applied load at the monopile head (Yang, 2018).

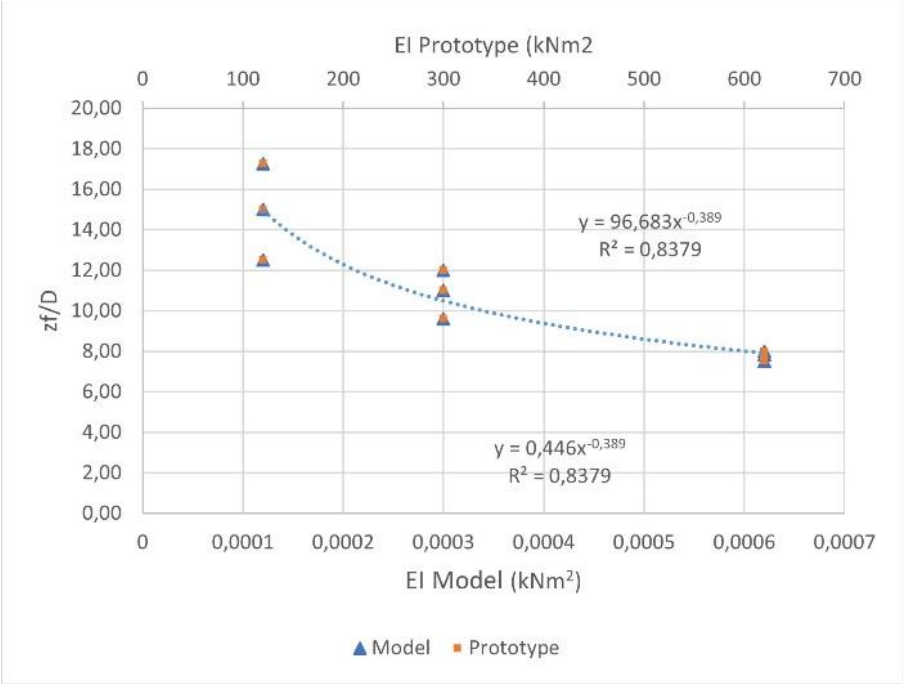

Figure 9. Application of Stiffness Values to Fixity Points

As shown in Figure 9, the graph illustrating the relationship between the EI Model and the fixity point ratio (Zf/D) indicates that as the flexural stiffness of the pile (EI) increases, the Zf/D ratio actually decreases. This suggests that as the stiffness of the pile increases, the fixity point forms at a relatively shallower depth.

At low EI values, the Zf/D ratio remains high, meaning the fixity point is deeper because the pile is more prone to deflection, thus requiring greater soil resistance at depth. Conversely, at higher EI values, the pile becomes stiffer, reducing lateral deflection and causing effective soil restraint to occur closer to the surface, resulting in a smaller Zf/D value.

The laboratory fixity point values range from 10.5D to 17.3D, and the theoretical values range from 14.1D to 19.2D. However, there is a difference with the research by Perumalsamy (2022), namely, the fixity point value ranges from 10D to 15D for sloping soil and 4D to 6D for flat soil. Also, research by Subhasinghe (2024) ranges from 0.5D to 2.5D. For L/D, the depth of fixity is nearly at 10.2D, 11.3D, and 10.4D (D = pile diameter) below the soil surface (Rathod, 2017).

In predominantly cohesive soils, depths of fixity determined from Broms method, Kocsis method, and p-y curves method vary between 1.5_{Dp} – 2.0_{Dp}, 1.0_{Dp} – 2.0_{Dp}, and 1.0_{Dp} – 1.5_{Dp} respectively. However, in predominantly cohesionless soils, depths of fixities determined by Broms method and p-y curves method vary between 1.0_{Dp} – 1.5_{Dp}, while the Kocsis method shows a slight variation of approximately around 1.5_{Dp} (Subhasinghe, 2024). For piles with D ≤ 1 m, a good agreement is demonstrated up to a lateral displacement of about 0.1D (Yang, 2016).

Eccentricity plays a significant role in influencing both the location of the fixity point and the magnitude of lateral deflection. The presence of load eccentricity generates additional bending moments, which amplify structural deformation and effectively reduce the overall stiffness of the system. As the eccentricity increases, the upper portion of the structural element experiences greater rotation, causing the effective fixity point to shift

deeper along the embedded length. An increase in eccentricity therefore leads to higher bending demand and a reduction in effective flexural stiffness. This shift in the fixity point directly affects the deflection response and alters the load-carrying mechanism of the structural element.

Tables 5 and 6 also present eccentricity values calculated using the ratio between the deflection value and the fixity point. These values are then plotted in the graphs shown in Figures 10 and 11 to illustrate the relationship between pile stiffness and the eccentricity ratio.

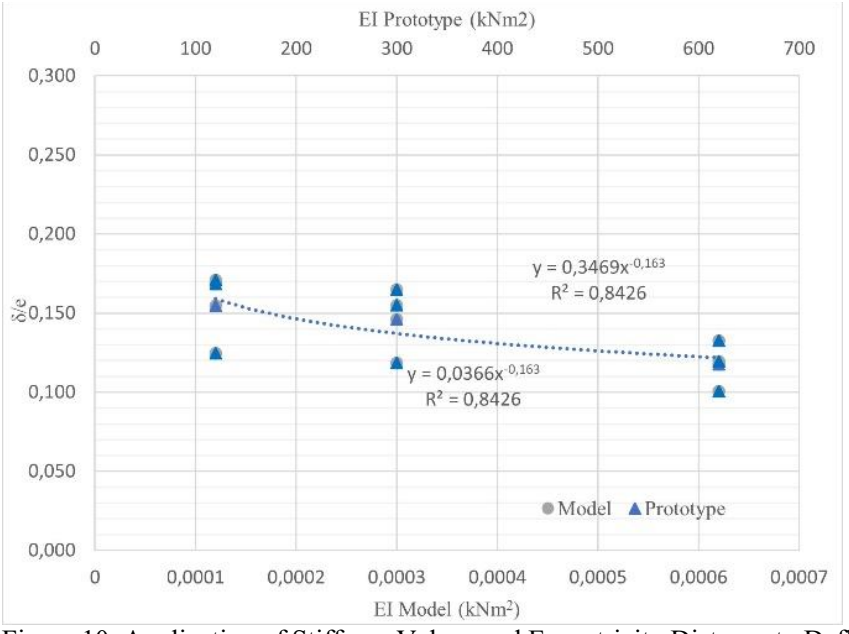

Figure 10. Application of Stiffness Values and Eccentricity Distance to Deflection Values

Figure 10 shows the relationship between the flexural stiffness of the pile (EI Model) and the deflection-to-eccentricity ratio (δ/e) under model and prototype conditions. The δ/e ratio describes the magnitude of the pile's lateral deflection response due to the eccentricity of the load acting on the pile head. Based on Figure 10, it can be seen that as the flexural stiffness (EI) increases, the deflection-to-eccentricity ratio decreases. This indicates that stiffer piles are better able to reduce the effect of load eccentricity, resulting in smaller lateral deformations. At low EI values, the δ/e ratio is relatively larger because the pile is more prone to bending due to the eccentric moment. Conversely, increased stiffness leads to improved flexural resistance, resulting in more controlled deflection. The deflection values range from 0.1e to 0.17e.

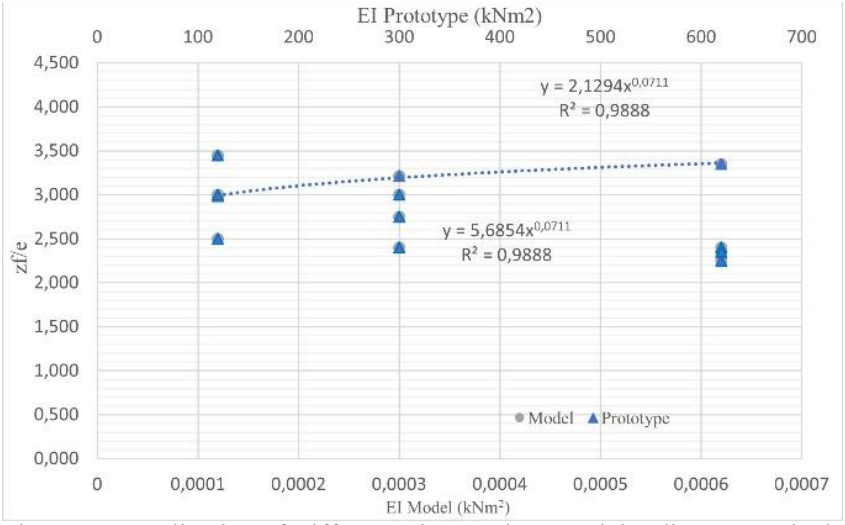

Figure 11. Application of stiffness values and eccentricity distance to the location of the fixity point

Based on Figure 11, the graph shows that an increase in the flexural stiffness (EI) causes the zf/e ratio to tend to increase, albeit by a relatively small amount. This indicates that stiffer piles are better able to withstand the effects of eccentricity, making the position of the fixed point relatively more stable against the influence of eccentric loading. In piles with low stiffness, the flexural response is greater, so the position of the fixed point is relatively more affected by load eccentricity. The fixity point values for laboratory and theoretical results are quite close. The fixity point values range from 2.5e to 3.6e.

Furthermore, the regression equations obtained from the experimental results can be extended to prototype-scale applications such as on Table 7. By using the structural flexural rigidity (EI) as the governing parameter, it is possible to predict the normalized values of δ/D, zf/D, δ/e, and zf/e. These dimensionless ratios provide a practical reference for estimating deflection and fixity point location in full-scale structures without the need for additional experimental testing. As lateral load increases, pile head displacement and maximum bending moment expand at a significantly faster rate (Jiang, 2018).

Table 7. Comparison of EI stiffness values

No.	Material	I (m^4)	E (kN/m^2)	EI (kNm^2)		EIp (kNm^2)
1	Beton D16	0.000032	23500000	755.6096	>	619.01
2	Beton D15	0.000025	23500000	583.69043	<	619.01
3	Beton D13	0.000014	23500000	329.299405	<	619.01
4	Beton D10	0.000005	23500000	115.296875	<	619.01
5	Beton 15 x 15	4.21875E-05	23500000	991.40625	>	619.01
6	Beton 14 x 14	3.20133E-05	23500000	752.313333	>	619.01
7	Beton 13 x 13	2.38008E-05	23500000	559.319583	<	619.01
8	Pipa baja D10	1.96399E-06	200000000	392.798928	<	619.01
9	Pipa baja D125	3.97864E-06	200000000	795.727653	>	619.01

Table 7 shows the calculation results for other foundation types and shapes, such as circular and rectangular, and other materials, such as steel. It can be seen that when compared to the elp threshold value of 619.01 kNm², some materials such as d16 concrete, 15 × 15 concrete, and d125 steel pipe exhibit higher stiffness (EI > 619.01 kNm²), while the rest fall below that value. Thus, figures 8 – 11 can be applied to other types of foundations.

CONCLUSION

Laboratory modeling tests show that the effect of column stiffness (EI) variation on deflection values for EI1 = 0.00012 kNm^2 ranges from 0.19D to 0.86D; EI2 = 0.0003 kNm^2 ranges from 0.16D to 0.66D, and EI3 = 0.00062 kNm^2 ranges from 0.09D to 0.44D. Image (photo) readings obtained fixity point values ranging from EI1 = 0.00012 $kNm^{2,}$ ranging from 12.5D to 17.3D; EI2 = 0.0003 $kNm^{2,}$ ranging from 12D to 14D, and EI3 = 0.00062 $kNm^{2,}$ ranging from 10.5D to 12D. The eccentricity distance affects the deflection value and the location of the fixity point for deflections ranging from 0.1e to 0.17e and fixity point locations ranging from 3e to 3.6e.

CONFLICTS OF INTEREST

The authors declare that there are no conflicts of interest regarding the publication of this paper.

REFERENCES

Abdelaziz, A. Y., El Naggar, M. H., & Ouda, M. (2021). Determination of depth-of-fixity point for laterally loaded vertical offshore piles: A new approach. *Ocean Engineering, 232*, 109113.

Bhuiyan, F. M., Motamed, R., & Siddharthan, R. V. (2024). An analytical approach to determine point-of-fixity of deep foundation utilizing nonlinear response from p-y analysis. In *Proceedings of Geo-Congress 2024 (GSP 350)*.

Boudaa, S., Khalfallah, S., & Bilotta, E. (2019). Static interaction analysis between beam and layered soil using a two-parameter elastic foundation. *International Journal of Advanced Structural Engineering, 11*(1), 21–30.

Darmawandi A., Waruwu A., Halawa T., Harianto D. dan Muammar. (2020). *Characteristics of Soft Soil in North Sumatra Based on*

Unconfined Compressive Strength Testing. Faculty of Civil Engineering and Planning, Medan Institute of Technology.

Deendayal, R., Muthukkumaran, K., & Sitharam, T. G. (2018). Analysis of laterally loaded group of piles located on sloping ground. *International Journal of Geotechnical Engineering*.

Gan, Y., Li, Y., Zhu, H., & Zhang, B. (2026). Probabilistic analysis of top deflection of laterally loaded piles considering spatially variable soil stiffness. *Computers and Geotechnics*, 189, 107592.

Hazzar, L., Hussien, M. N., & Karray, M. (2017). On the behaviour of pile groups under combined lateral and vertical loading. *Ocean Engineering*, 131, 174–185.

Jagtap, S. S., Rasal, S. A., & Dode, P. A. (2017). Analysis of depth of fixity for pile groups. *International Journal of Civil Engineering and Technology (IJCIET)*.

Jegatheeswaran, B., & Muthukkumaran, K. (2016). Behavior of pile due to combined loading with lateral soil movement. *International Journal of Geo-Engineering, 7*(8).

Jeong, S., and Kim, Y. (2020). "Analysis for laterally loaded offshore piles in marine clay." *Geotechnical Engineering*, 51(2), 166-171.

Jiang, C., He, J.-L., Liu, L., & Sun, B.-W. (2018). Effect of loading direction and slope on laterally loaded pile in sloping ground. *Advances in Civil Engineering*, 2018, Article ID 7569578, 12 pages.

Kavitha, P. E., Beena, K. S., & Narayanan, K. P. (2016). A review on soil–structure interaction analysis of laterally loaded piles. *Innovative Infrastructure Solutions*, 1(1), Article 14.

Li, Q., Prendergast, L. J., Askarinejad, A., & Gavin, K. (2020). Influence of vertical loading on behavior of laterally loaded foundation piles: A review. *Journal of Marine Science and Engineering*, 8(12).

Lu, W., & Zhang, G. (2018). Influence mechanism of vertical-horizontal combined loads on the response of a single pile in sand. *Soils and Foundations*, 58, 1228–1239.

Moayedi, H., Nazir, R., Mosallanezhad, M., Noor, R. B. M., & Khalilpour, M. (2018). Lateral deflection of piles in a multilayer soil medium: Case study: The Terengganu seaside platform. *Measurement, 123*, 185–192.

Mu, L., Kang, X., Feng, K., Huang, M., & Cao, J. (2017). Influence of vertical loads on lateral behaviour of monopiles in sand. *European Journal of Environmental and Civil Engineering*.

Nimityongskul, N., Kawamata, Y., Rayamajhi, D., & Ashford, S. A. (2018). Full-scale tests on effects of slope on lateral capacity of piles installed in cohesive soils. *Journal of Geotechnical and Geoenvironmental Engineering,* 144(1), 04017103.

Perumalsamy, K., & Ranganathan, S. (2022). Single pile in cohesionless soil in sloping ground under lateral loading. *International Journal of Geo-Engineering*, (13), 8.

Rad, M. M. (2017). Reliability based analysis and optimum design of laterally loaded piles. *Periodica Polytechnica Civil Engineering,* 61(3), 491–497.

Rathod, D., Muthukkumaran, K., & Sitharam, T. G. (2017). Development of non-dimension p–y curves for laterally loaded piles in sloping ground. *Indian Geotechnical Journal*, 47(1), 47–56.

Rawung C. T., Sumanpouw, Josef E.R dan Oktavian B. A. Sompie. (2020). Analysis of Eccentric Lateral Load Behavior on the Capacity of Single Vertical Piles in Homogeneous Sand. *Jurnal Sipil Statik*, 8 (6), 2337-6732.

Sazzad, M. M., Ashikuzzaman, M., Roni, M. A. U., & Ahamed, M. (2019). Effect of length-to-diameter ratio on the load-deflection characteristics of laterally loaded driven piles in sand. *Proceedings of the International Conference on Planning, Architecture and Civil Engineering*, Rajshahi University of Engineering & Technology, Rajshahi, Bangladesh.

Subhasinghe, R. M. K. R., & de Silva, L. I. N. (2024). Applicability of analytical methods to estimate the point of fixity of laterally loaded piles on multilayered soils. In *Proceedings of the Annual Sessions of the Institution of Engineers, Sri Lanka (IESL)* (15–22).

Subhasinghe, R. M. K. R., & De Silva, L. I. N. (2024). *Point of fixity of laterally loaded piles on layered soils.* Civil Engineering Research Symposium 2024, Department of Civil Engineering, University of Moratuwa, Moratuwa.

Yang, M., Ge, B., & Li, W. (2018). Force on the laterally loaded monopile in sandy soil. *European Journal of Environmental and Civil Engineering*.

Yang, M., Ge, B., Li, W., & Zhu, B. (2016). Dimension effect on P–y model used for design of laterally loaded piles. *Procedia Engineering, 143*, 598–606.

Yin, P., He, W., & Yang, Z. J. (2018). A simplified nonlinear method for a laterally loaded pile in sloping ground. *Advances in Civil Engineering*, 2018, Article ID 5438618, 9 pages.

Yin, Pingbao., He Wei., & Yang Z.J. (2018). *A Simplified Nonlinear Method for a Laterally Loaded Pile in Sloping Ground*. School of Civil Engineering, Changsha University of Science and Technology, Changsha 410114, China.

Yuan, B., Xu, K., Wang, Y., Chen, R., & Luo, Q. (2017). Investigation of deflection of a laterally loaded pile and soil deformation using the PIV technique. *International Journal of Geomechanics*, 17(6), 04016138.

Zhang, X.-l., Xue, J.-y., Xu, C.-s., & Liu, K.-y. (2021). An analysis method for lateral capacity of pile foundation under existing vertical loads. *Soil Dynamics and Earthquake Engineering, 142*, 106547.

Zhang, Y., & Andersen, K. H. (2017). Scaling of lateral pile p-y response in clay from laboratory stress-strain curves. *Marine Structures, 53*, 124–135.

Zhao T. & Wang Yu. 2018. *Interpretation Of Pile Lateral Response From Deflection Measurement Data: A Compressive Sampling-Based Method*. Department of Architecture and Civil Engineering, City University of Hong Kong Tat Chee Avenue Kowloon Hong Kong, (58), 957-971.